

Mizuyasu Koide · Tsutomu Takahashi · Masataka Shirakashi · Sheikh Ahmad Zaki Bin Shaikh Salim

Three-dimensional structure of longitudinal vortices shedding from cruciform two-cylinder systems with different geometries

Received: 9 June 2016 / Revised: 27 December 2016 / Accepted: 16 January 2017 / Published online: 16 February 2017
© The Visualization Society of Japan 2017

Abstract In previous research the present authors have shown that cross flow vibrations can be induced on a cylinder by setting another cylindrical body downstream in cruciform arrangement with a certain gap s between them. These vibrations are excited by two longitudinal vortices (LVs), i.e. the trailing vortex (TV) and the necklace vortex (NV), shedding periodically near the cross of the system. In this study, LVs shedding from three cruciform systems, i.e. circular-cylinder/circular-cylinder (CC/CC), circular-cylinder/strip-plate (CC/SP) and square-cylinder/strip-plate (SC/SP) system, are observed from three directions using water tunnel and surface-dye-streak technique to clarify their three-dimensional structure. The gap-to-diameter ratio s/d is set at 0.08 or 0.28 as the representative values of TV and NV, respectively. Formation of TV or NV depends on the system geometry s/d and Reynolds number Re . In the case of CC/CC, TV is formed at $s/d = 0.08$ and NV at $s/d = 0.28$ steadily when $1400 \leq Re \leq 2000$, and they shed periodically when $3300 \leq Re \leq 5700$. In the case of CC/SP, steady shedding of TV is observed at the both values of s/d in the lower Re range and periodic shedding is observed only for TV at $s/d = 0.08$ in the higher Re range, but with poorer periodicity. In the case of SC/SP, NV is formed at the both values of s/d and periodic shedding is not observed up to the highest value of $Re = 5000$ in this experiment.

Keywords Cruciform two-cylinder system · Longitudinal vortex · Trailing vortex · Necklace vortex · Dye ejection · Transition

1 Introduction

As early as 1989, the present authors investigated the influence of an equal diameter downstream cylinder in cruciform arrangement on the vibration of a circular cylinder in air flow, and confirmed that the cross flow mode Kármán vortex induced vibration (KVIV) is effectively suppressed by the downstream cylinder when

M. Koide (✉)

Department of Mechanical Engineering, National Institute of Technology, Fukushima College,
30 Taira Kamiarakawa Nagao, Iwaki, Fukushima 970-8034, Japan
E-mail: mkoide@fukushima-nct.ac.jp

T. Takahashi

Department of Mechanical Engineering, Nagaoka University of Technology, 1603-1 Kamitomioka,
Nagaoka, Niigata 940-2188, Japan

M. Shirakashi

Professor Emeritus, Nagaoka University of Technology, 1603-1 Kamitomioka, Nagaoka, Niigata 940-2188, Japan

S. A. Z. B. S. Salim

Department of Mechanical Precision Engineering, Malaysia-Japan International Institute of Technology,
Universiti Teknologi Malaysia, Jalan Semarak, 54100 Kuala Lumpur, Malaysia

the gap-to-diameter ratio $s/d < 0.5$ (Shirakashi et al. 1989; Bae et al. 2001). However, at the same time, it was found that other vibrations are induced over higher velocity ranges. Later wind tunnel experiments on the flow around fixed cruciform circular-cylinder/circular-cylinder (CC/CC) system supported by visualization in water tunnel showed that the newly found vibrations are caused by two longitudinal vortices (LVs) as shown in Fig. 1a, the trailing vortex (TV) and the necklace vortex (NV), which shed periodically near the cross generating alternating lift force acting on the upstream cylinder (Shirakashi et al. 1994, 2001; Takahashi et al. 1999). Since the two LVs can synchronize with the cylinder oscillation resulting in resonance-like vibrations over wide velocity ranges, like the case of the KVIV, they are called trailing vortex induced vibration (TVIV) and necklace vortex induced vibration (NVIV), and collectively longitudinal vortex induced vibration (LVIV). It was also shown that the vibration amplitude of TVIV and NVIV are largest at $s/d = 0.08$ and 0.28 , respectively.

Later, it was shown that periodic shedding of LVs occurs over wide range of conditions for fixed CC/CC (Nguyen et al. 2010). Accordingly, the LVIVs are also observed over wide range of conditions. For CC/CC, Shirakashi et al. (2001) reported that the two LVIVs can occur for systems with the diameter ratio of downstream to upstream cylinder $d_2/d_1 = 0.5-2$. Nguyen et al. (2012) showed that TVIV of CC/CC with a comparable Scruton number ($=2 \times \text{mass ratio} \times \text{logarithmic damping factor}$) occurs in water flow over the same range of reduced velocity, while the similarity of NVIV between in water and air flow is less clear.

Recently, Kato et al. (2012) carried out wind tunnel experiments on LVIVs of a circular-cylinder/strip-plate system (CC/SP) in which the downstream fixed circular cylinder is replaced by a strip plate with a width w . They reported that the two LVIVs occur for CC/SP with $w/d \leq 0.6$ over respective ranges of s/d while NVIV is not clearly observed when $w/d \geq 1.0$. Koide et al. (2007) and Kawabata et al. (2013) carried out wind tunnel experiment on LVIVs of a square-cylinder/strip-plate system (SC/SP) in which the circular cylinder in CC/SP is replaced by a square cylinder with a side length equal to the cylinder diameter. In this case, an LVIV of square cylinder is induced by the strip plate, which they considered to be attributable to TV.

Flow around fixed CC/CC with $s/d = 0$, i.e. the two cylinder are in contact, was observed by Zdravkovich (1983), who confirmed that a TV having its foot on the upstream cylinder surface forms steadily at each corner of the cross. Takahashi et al. (1999) investigated influence of s/d on LVs for CC/CC, and showed that TV and NV shown in Fig. 1a shed periodically when $s/d < 0.25$ and $0.25 < s/d < 0.5$,

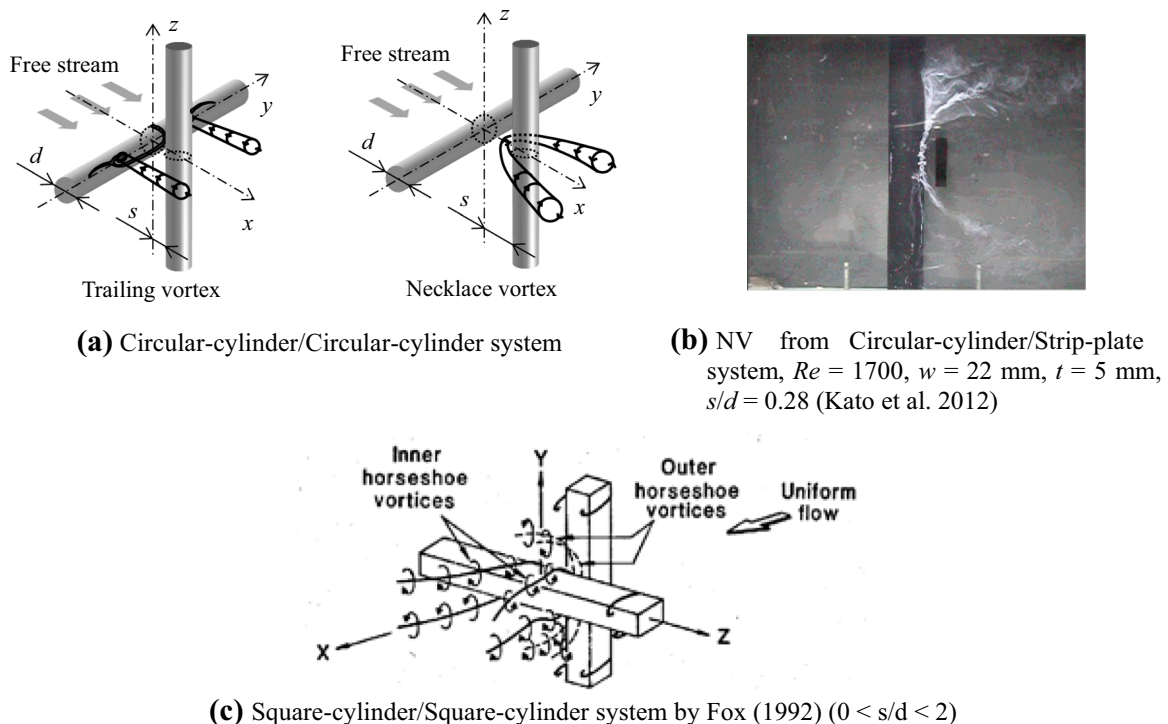


Fig. 1 Longitudinal vortices shedding from cruciform systems

respectively. It is also shown that the periodicity of TV and NV shedding is most regular at 0.08 and 0.28, respectively, in consistent with the results on LVIVs described above.

Although NVIV was not observed for CC/SP with $w/d = 1$, the two LVs are observed to form steadily for this system when Reynolds number Re is as low as 1800, as seen in Fig. 1b (Kato et al. 2012).

Fox (1992) observed “Inner and Outer horseshoe vortices” shedding from cruciform two identical square cylinder system with $s/d = 0-2$ as shown in Fig. 1c. This vortex regime is considered to be almost equivalent to the case of SC/SP since influence of the thickness of the strip-plate is insignificant.

The results on LVIVs and observations on the structure of flow around fixed counterpart systems seem consistent for CC/CC, while they are inconsistent for CC/SP and SC/SP. In this study, the longitudinal vortices shedding from the aforementioned three fixed cruciform systems are observed using water tunnel and surface-dye-streak technique, to clarify the differences in structure of LVs over the range of Re where the transition from steady to periodic shedding may occur. For this purpose, a water tunnel was designed and constructed to enable observation from three directions.

2 Experimental apparatus and procedure

A water tunnel designed for flow visualization experiment was used in order to observe the longitudinal vortices from three directions, i.e. from the side, the bottom and the downstream. The measuring section has a square cross section with 200 mm sides and a 500 mm length. The velocity profile has uniform core extending over 93% of vertical and horizontal widths. The velocity, U , of the uniform core region is determined from the flow rate Q measured by an electromagnetic flow meter as $U = c(Q/A)$, where A is the cross sectional area of the measuring section and the coefficient $c = 1.05$ is determined by calibration experiments. The stream-wise turbulence intensity is less than 3% over the experimental range of U .

A circular cylinder with a diameter $d = 20$ mm or a square cylinder with a side length $d = 20$ mm was spanned horizontally at the center of the measuring section, fixed to the side walls. The origin of coordinate system $O-(x, y, z)$ used in this paper is set at the center of the upstream cylinder as shown in Fig. 1a. For visualization, dyed water with neutrally-buoyant density was ejected from 1.0 mm diameter nine holes on the cylinder surface shown in Fig. 2. In this paper, three holes on the generating lines at $(x/d = 0, z/d = 0.5)$, $(x/d = 0.5, z/d = 0)$ and $(x/d = 0, z/d = -0.5)$ are called as top, center and bottom holes, respectively. For CC/CC, a circular cylinder with a diameter $d = 20$ mm was set vertically downstream the first cylinder to form cruciform system, while for CC/SP and SC/SP a strip-plate with a width $w = 20$ mm and thickness $t = 5$ mm was used as the downstream body. The gap ratio s/d was set at 0.08 or 0.28 since these are respective representative values of TV and NV for CC/CC. These conditions, together with the experimental ranges of U and Re are given in Table 1.

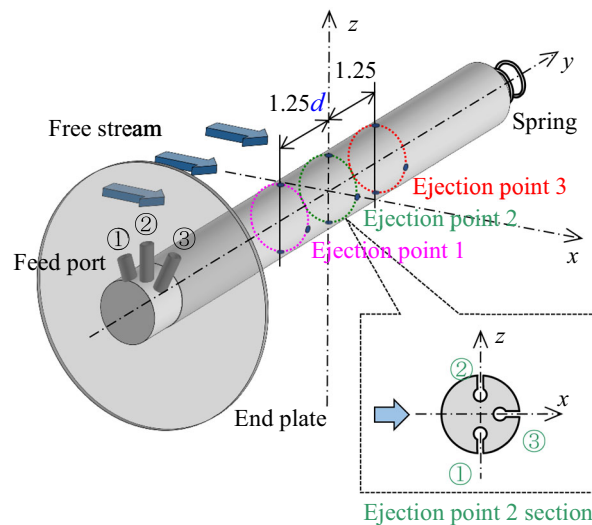
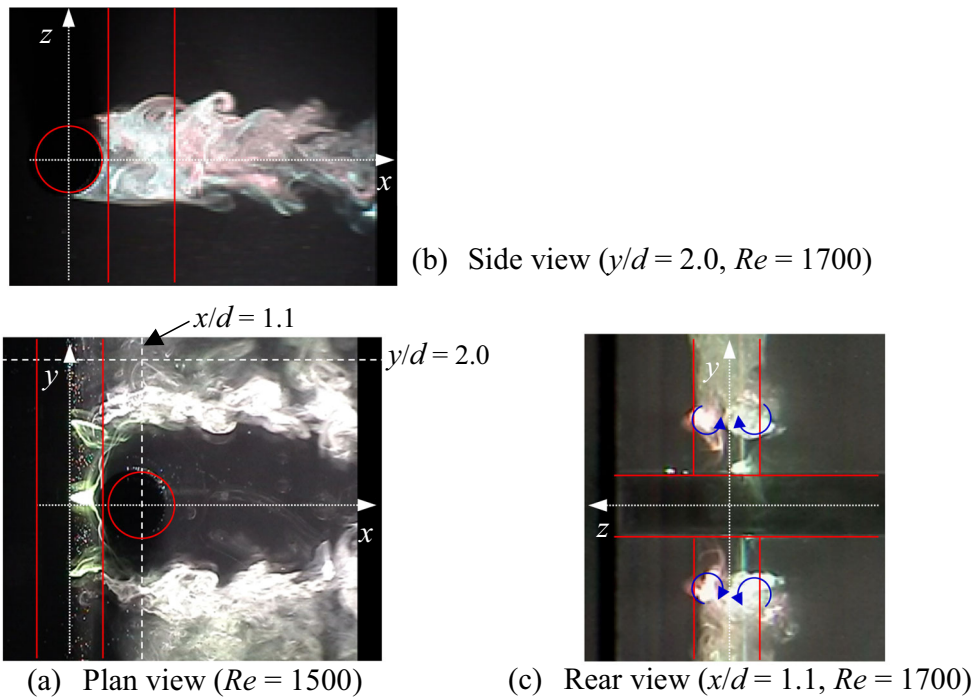


Fig. 2 Location of die ejection holes on the upstream cylinder

Table 1 Dimensions of the cruciform two-cylinder systems

Test system	CC/CC	CC/SP	SC/SP
Upstream object size (mm)	$d = 20$ $l = 197$		$d = 20$ $l = 197$
Downstream object size (mm)	$d = 20$	$w = 20$ $t = 5$	
s/d	0.08, 0.28		
U (m/s)	0.08, 0.10, 0.20, 0.30		
$Re = Ud/\nu$	1200–5700		

l cylinder length, ν kinematic viscosity

**Fig. 3** TV for CC/CC with $s/d = 0.08$ at low Re

Plan view photographs were taken from the bottom, i.e. from negative z -direction, of the measuring section using a mirror, thus the reflected images are presented in this paper. Cross sections of LVs at constant values of y - or x -coordinate were visualized by 2 mm thickness light sheet. The side view photographs on y -constant planes were taken from negative y -direction, while the rear view photographs on x -constant planes were taken from downstream viewed down by an angle of 20° from the x -axis.

For the plan view photography, green dye was ejected from the bottom holes and white dye from the center holes in the cases of CC/CC and CC/SP, while green and red, respectively, in the case of SC/SP. For the side view of y -constant plane and the rear view of x -constant cross section, red dye from top holes and green dye from the bottom holes were ejected. In Figs. 3, 4, 5, 6, 7 and 8, photographs thus obtained are reproduced in an equal scale and the contour of the upstream cylinder and the cross section of the downstream object on the $z = 0$ plane is indicated by red line.

3 Observation of vortex structure

3.1 Longitudinal vortices with $s/d = 0.08$ at low Reynolds number

The three directional views at the lowest Reynolds number range in this experiment, i.e. $Re = 1500$ – 1800 , for the three systems with $s/d = 0.08$ are presented in Figs. 3, 4 and 5. In the plan view of Fig. 3a for CC/

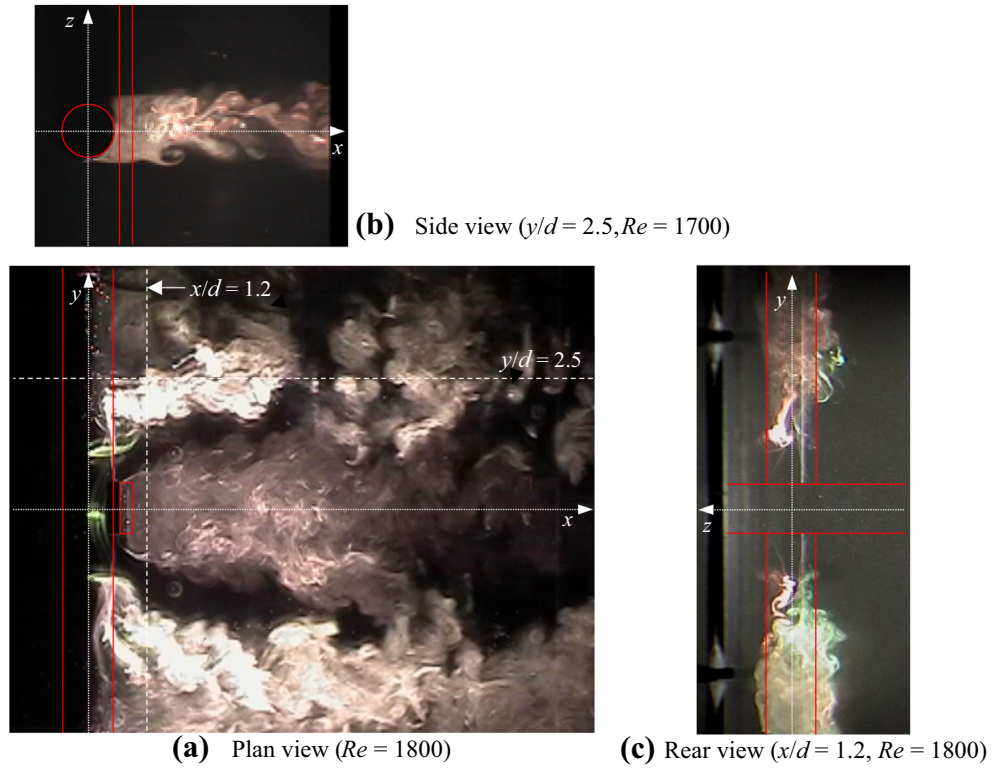


Fig. 4 TV for CC/SP with $s/d = 0.08$ at low Re

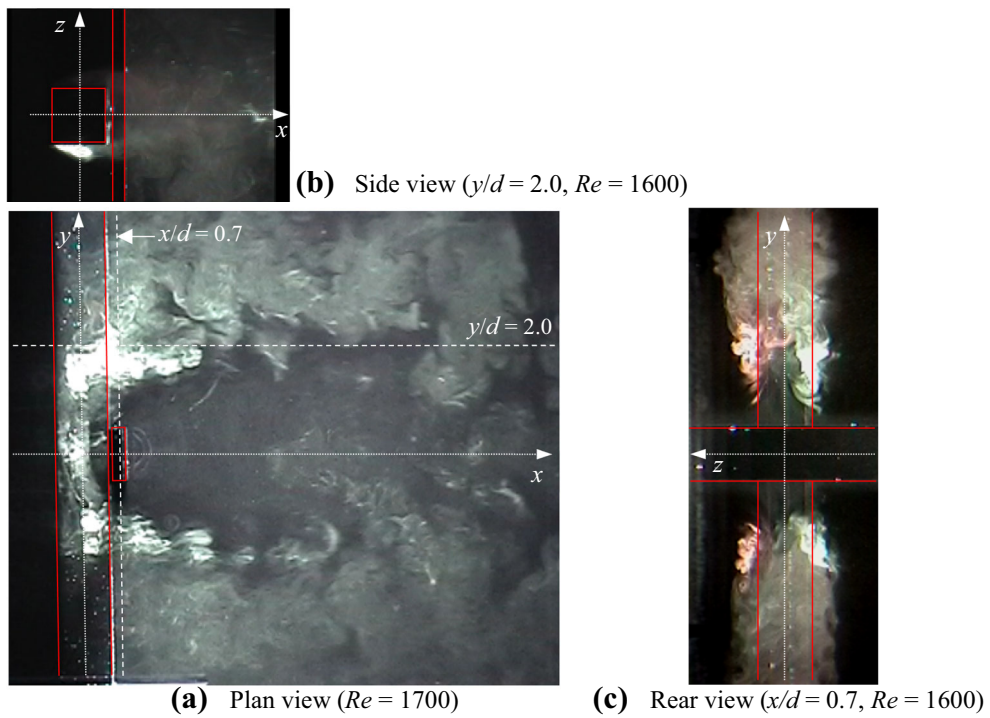


Fig. 5 Photographs of LV for SC/SP with $s/d = 0.08$ at low Re

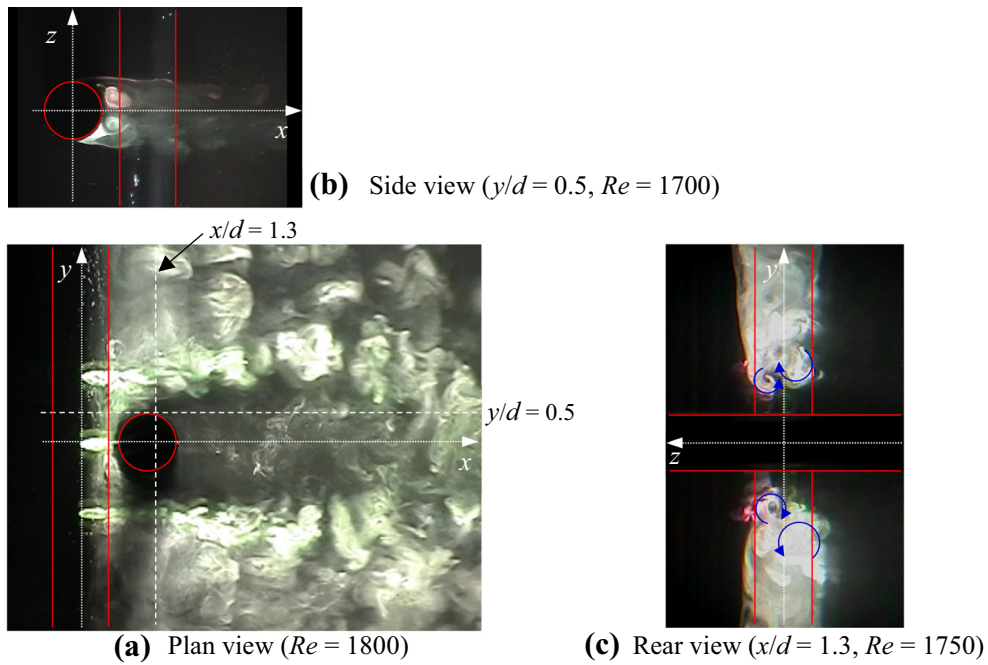


Fig. 6 Photographs of NV for CC/CC with $s/d = 0.28$ at low Re

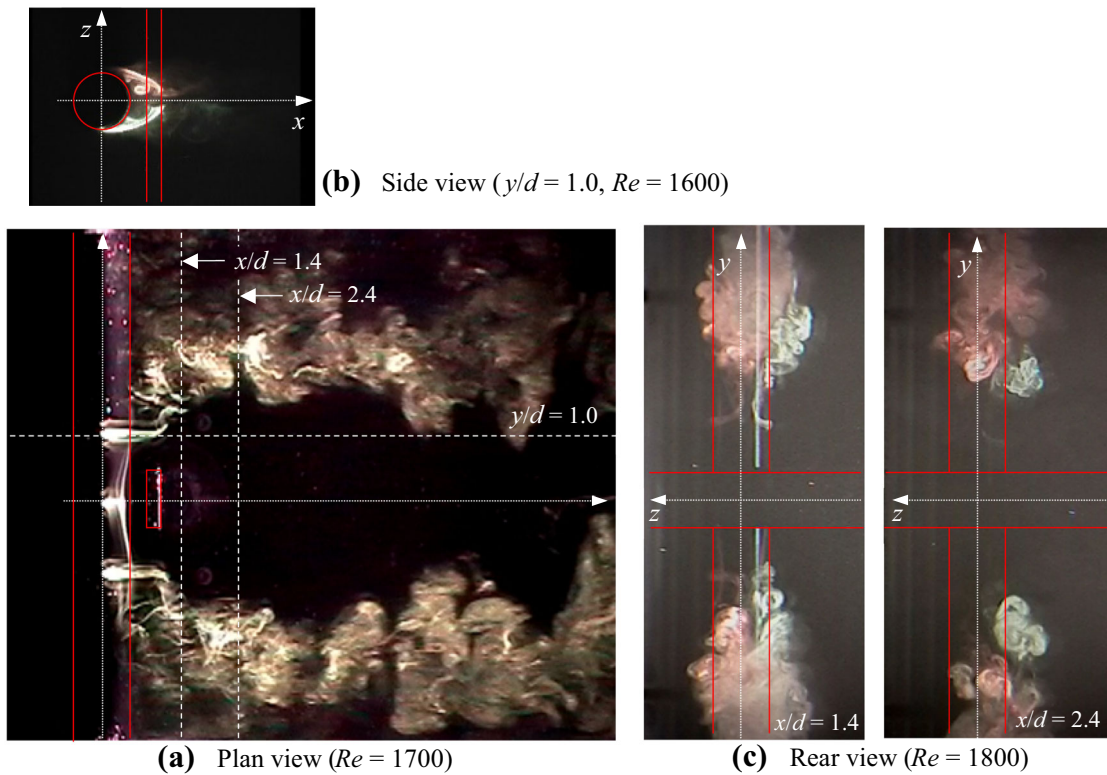


Fig. 7 Photographs of LV for CC/SP with $s/d = 0.28$ at low Re

CC, dyed fluid between the cylinders flows along the downstream stagnation line of the upstream cylinder separating from the $y = 0$ plane, and is drawn into two tornado-like trailing vortices symmetric about the $y = 0$ plane with axes almost parallel to the x -axis. Four TVs exist simultaneously and symmetric about the

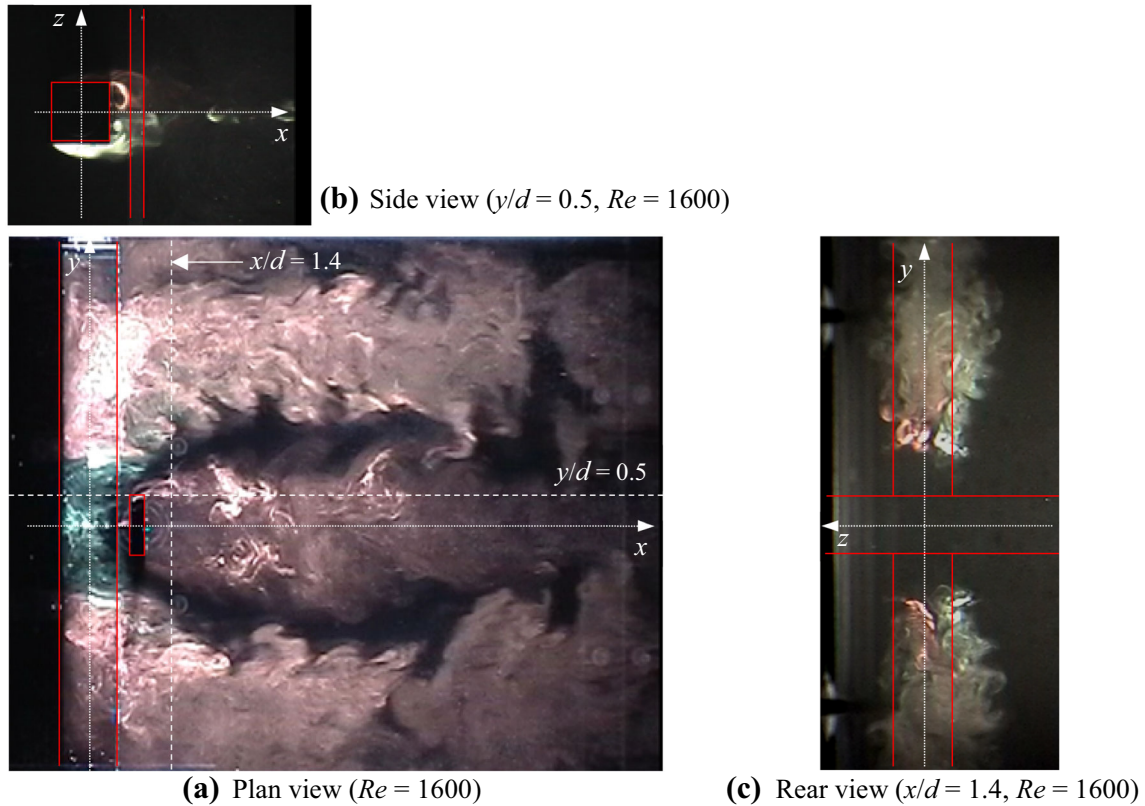


Fig. 8 Photographs of LV for SC/SP with $s/d = 0.28$ at low Re

$y = 0$ and $z = 0$ planes as seen in Fig. 3c. They are formed stably and steadily with their axis located around $|y/d| = 2.0$ as seen in Fig. 3a, and their longitudinal cross section is shown in Fig. 3b.

In the case of CC/SP with $s/d = 0.08$, the trailing vortices are formed similarly at low Re but the axis is definitely curved near the upstream cylinder before becoming parallel to the x -axis, as seen by comparing Fig. 4a with Fig. 3a. Compared with CC/CC, the trailing vortex of CC/SP is significantly unstable in size and accompanied by an irregular movement of its axis in y -direction. Generally speaking, the separation of the axes in the downstream parallel part is considerably larger than that of CC/CC, say $|y/d| = 2.5$ as seen in Fig. 4a. The irregular feature is clearly observed in the rear view in (c), which shows that the four trailing vortices at each corner of the cross have no clear contour and are considerably different in size with respect to each other.

The vortex structure of SC/SP with $s/d = 0.08$ shown in Fig. 5 is quite different from the other two systems. In (a) the trailing vortex is not observed but the dyed water ejected from the bottom holes directly rolls into a vortex wrapping the downstream strip plate to form the necklace shape pattern detaching the plate. This is consistent with Fox's observation of "outer horseshoe vortex" in Fig. 1c. In the side view of the $y/d = 2.0$ plane in Fig. 5b, a flat vortex pattern is observed on the lower side of the square showing the cross section of NV. The rear view in (c) shows that a pair of necklace vortices is formed symmetrically about the $z = 0$ plane. The formation of the NV under this condition is as stable as the case of TV in Fig. 3.

3.2 Longitudinal vortices with $s/d = 0.28$ at low Reynolds numbers

In Figs. 6, 7 and 8, s/d is set at 0.28 while the other conditions are correlating with the previous section. Figure 6 for CC/CC shows three dimensional structure of NV shown in Fig. 1a. In the plan view (a), dye streak from the bottom holes rolls into a vortex around the downstream cylinder. The gap between the NV and the downstream body in this photograph is significantly smaller than the case of SC/SP with $s/d = 0.08$ in Fig. 5a. The distance of the axes of the two branches of NV at $x/d > 3$ is smaller than that of the trailing vortex axes in Fig. 3a. That is, the position of the axis of NV at $x/d > 3$ is $|y/d| \sim 1.5$. The

photograph of the $y/d = 0.5$ cross section in Fig. 6b clearly shows a pair of vortex pattern in the gap between the cylinders, which confirms that a pair of NV is formed simultaneously on both sides of the $z = 0$ plane. The rear view in (c) shows that the shape of the NV is similar to that observed for SC/SP at $s/d = 0.08$ in Fig. 5c, but not so symmetric about the $z = 0$ plane.

The shape of the vortex for CC/SP in Fig. 7a is similar to that of CC/CC in Fig. 6a, showing that the dye streak separating from the surface of the cylinder rolls into NV around the strip-plate. The side view for $y/d = 1.0$ in Fig. 7b shows a pair of vortex pattern symmetric about the $z = 0$ plane confirming formation of NV. However, this flow pattern is very unstable and frequently replaced by the TV regime similar to that shown in Fig. 4. In the left photograph of Fig. 7c, cross sections of four TVs are observed. While, in the right photograph, the pattern is symmetric about the $y = 0$ plane, but the distance of the vortex pair in the upper side ($z > 0$) is considerably larger than that of the lower ($z < 0$) side. Since the former is correlated with TV and the latter with NV, Fig. 7 indicates simultaneous formation of TV and NV. Thus, NV regime is not dominantly established for CC/SP with $s/d = 0.28$, unlike the case of CC/CC.

For SC/SP shown in Fig. 8, an NV is observed on the upper side of the square cylinder in the plan view (a), which corresponds with the “outer horseshoe vortex” in Fig. 1c reported by Fox for a square-cylinder/square-cylinder system. The cross section on the $y/d = 0.5$ plane in Fig. 8b shows two different vortex patterns, one on the lower side surface of the square cylinder and the other in the gap between the square cylinder and the strip plate. The former corresponds to the “outer horseshoe vortex” and the latter to the “inner horseshoe vortex” reported by Fox (see Fig. 1c). The rear view in Fig. 8c shows that the NVs from SC/SP with $s/d = 0.28$ are formed steadily and symmetric about the $z = 0$ plane.

3.3 Behavior of LVs with increasing Re and correlation with LVIVs

3.3.1 CC/CC

TV shedding from CC/CC with $s/d = 0.08$ remains steady nature when $1400 < Re < 2000$, and irregular motion such as movement of the foot of TV in y -direction appears and becomes more unstable with increasing Re until it attains the periodic shedding phase at $Re > 3300$. It is observed that TV on this stage sheds alternately on the upper and lower side of the upstream cylinder as shown in Fig. 9, in consistent with the previous works. However, in this experiment it is sometimes observed that two TVs at diagonal positions shed periodically in phase as shown in Fig. 10. These two patterns of vortex shedding are observed more clearly by the attached movie video images.

Transition of NV from steady to periodic shedding for CC/CC at $s/d = 0.28$ as shown in Fig. 11 is observed with increasing Re from 1800 to 3500, similar to the above mentioned case of TV. It is observed that the NV at a side of upstream cylinder does not vanish when NV on the other side is in its maximum.

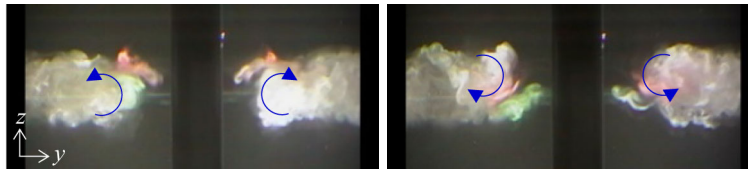


Fig. 9 Alternating shedding of TV from CC/CC with $s/d = 0.08$ at $Re = 3600$ symmetric about the $y = 0$ plane, rear view at $x/d = 1.1$

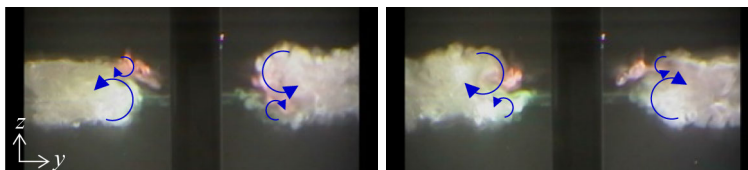


Fig. 10 Diagonal shedding of TV from CC/CC with $s/d = 0.08$ at $Re = 3600$, rear view at $x/d = 1.1$

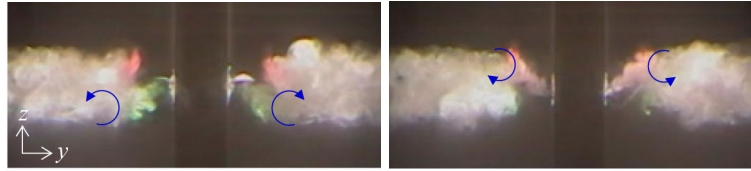


Fig. 11 Alternating shedding of NV from CC/CC with $s/d = 0.28$ at $Re = 3550$, rear view at $x/d = 1.3$

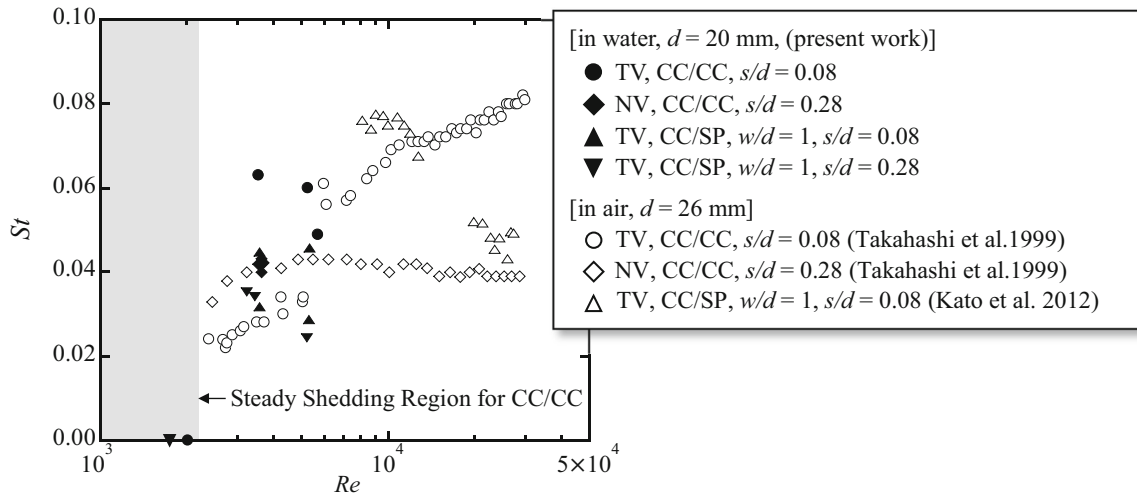


Fig. 12 Relationship between St and Re

The periodicity of the two longitudinal vortices is considerably regular and their frequency f_v is obtained by counting the number of vortex patterns appearing during a time interval. Then, f_v is converted into the Strouhal number $St = f_v d/U$ and plotted against Re in Fig. 12 compared with the results of previous works. In Fig. 12, transitions of TV and NV from steady to periodic shedding for CC/CC are clearly observed. As seen in Fig. 12, $St = 0$ both for TV and NV when $Re < 2000$, and $St = 0.05\text{--}0.06$ for TV and $St \sim 0.04$ for NV when $3500 < Re < 5000$. This result fairly agrees with the previous data in spite of the fact that the number of data in averaging in this work is much smaller than the measurement of wind tunnel experiment using HWA or load cell for lift force.

3.3.2 CC/SP

In the case of CC/SP with $s/d = 0.08$, the irregular motion of the trailing vortex observed in the lowest range of Re , i.e. $Re = 1400\text{--}1800$, becomes larger with increasing Re and attains periodic phase when $3200 \leq Re \leq 5400$ similar to the case of CC/CC in Fig. 9. However, the regularity of the periodic shedding is considerably poor compared with the case of CC/CC.

Although NV was clearly observed for CC/SP with $s/d = 0.28$ at $Re = 1700$ in the previous work, this work showed that NV is not stable due to coexistence of TV and dominated by unstable or periodic TV with increasing Re . That is, the NV observed at the lowest Re vanishes with increasing Re and TV sheds alternately from the upper and the lower side of the cylinder when $3200 \leq Re \leq 5400$. However, its periodicity is considerably irregular, like the case of $s/d = 0.08$. The vanishing of NV at the larger Re range is consistent with the wind tunnel experiment by Kato et al. (2012) reporting that NVIV does not occur for CC/SP with $w/d = 1$ and $s/d = 0.28$ for the elastic counterpart, unlike the case of CC/CC.

In spite of the irregularity of TV shedding, f_v was measured in the same way as applied to CC/CC. St thus obtained is also plotted in Fig. 12. The values of St for TV are scattered over the range $0.02\text{--}0.05$ in the measurement range of Re . Agreement of this result with the existing wind tunnel data is poor, may be due to the irregular nature of TV and rather small number of data in averaging.

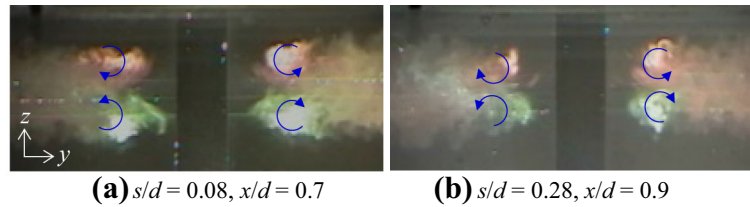


Fig. 13 Necklace vortex for SC/SP at $Re = 3300$, rear view

3.3.3 SC/SP

For SC/SP, the NVs observed at $s/d = 0.08$ and 0.28 remain steady and symmetric about the $z = 0$ plane up to the maximum value of Re in this experiment as seen in Fig. 13. This seems inconsistent with the previous works by Kawabata et al. (2013) in which the LVIV occurring at $s/d \sim 1.2$ is attributed to TV. At $s/d = 0.28$, it is observed that the two NVs shedding on the same side of square cylinder merges into one to form longitudinal vortices resembling the TV on both sides of the strip plate. Observation in this work tells that visualization experiment will be necessary to investigate the dependence of vortex structure on s/d , especially around $s/d = 1.2$ and higher Re range, to identify the vortices inducing LVIVs of SC/SP.

4 Concluding remarks

Observation of LVs on three cruciform systems with different geometries showed that the steady LVs are commonly formed when $Re < 1800$. However, their configurations and behaviors with increasing Reynolds number are different among them.

4.1 CC/CC

When $1400 < Re < 2000$, four TVs and two NVs are formed steadily at $s/d = 0.08$ and 0.28 respectively. They become unstable when $2500 < Re < 3300$, and shed periodically when $3300 < Re < 5700$. However, in this periodic region, it was found that TVs can shed in phase at diagonal positions of the cross. The relationship between the vortex shedding frequency and the flow velocity for TV and NV are shown to be consistent with the earlier wind tunnel experiments by reducing them into St and Re .

4.2 CC/SP

At $s/d = 0.08$, TV is formed steadily, but a little unstable when $1400 < Re < 2000$. With increasing Re , unstable motion becomes more violent until periodic phase is attained at $Re = 3000$, although it is not so regular as the case of CC/CC. At $s/d = 0.28$ and $Re \leq 1800$, both TV and NV are observed to be coexisting in some cases, unlike the case of CC/CC. With increasing Re , the shedding of TV becomes dominant and NV is not observed when $Re > 3000$.

4.3 SC/SP

At $s/d = 0.08$, an NV is formed steadily on each side of the square cylinder when $Re < 1800$, but TV is not observed unlike the cases of CC/CC and CC/SP. At $s/d = 0.28$, two different NVs are formed, corresponding to the inner and outer horseshoe vortex reported by Fox (1992) for the square-cylinder/square cylinder system.

When Re is increased, irregular motion appears like the other two systems at the both values of s/d , but NV shedding does not attain periodic phase at the maximum value of Re in this experiment.

Acknowledgements The authors express gratitude to Mr. Fumihito Kitamura for his contribution in performing the wind tunnel experiments. This research was financially supported by the Malaysian Ministry of Higher Education (MoHE) under the Fundamental Research Grant Scheme (4F479) project of Universiti Teknologi Malaysia.

References

- Bae HM, Baranyi L, Koide M, Takahashi T, Shirakashi M (2001) Suppression of Kármán vortex excitation of a circular cylinder by a second cylinder set downstream in cruciform arrangement. *J Comput Appl Mech* 2(2):175–188
- Fox TA (1992) Interference in the wake of two square-section cylinders arranged perpendicular to each other. *J Wind Eng Ind Aerodyn* 40(1):75–92. doi:[10.1016/0167-6105\(92\)90522-C](https://doi.org/10.1016/0167-6105(92)90522-C)
- Kato N, Koide M, Takahashi T, Shirakashi M (2012) VIVs of a Circular Cylinder with a downstream strip-plate in cruciform arrangement. *J Fluids Struct* 30:97–114. doi:[10.1016/j.jfluidstructs.2012.02.007](https://doi.org/10.1016/j.jfluidstructs.2012.02.007)
- Kawabata Y, Takahashi T, Haginoya T, Shirakashi M (2013) Interference effect of downstream strip-plate on the cross flow vibrations of a square cylinder. *J Fluid Sci Technol* 8(3):348–363. doi:[10.1299/jfst.8.348](https://doi.org/10.1299/jfst.8.348)
- Koide M, Kato N, Yamada S, Kawabata Y, Takahashi T, Shirakashi M (2007) Influence of a cruciform arrangement downstream strip plate on crossflow vibration of a square cylinder. *J Comput Appl Mech* 8(2):135–148
- Nguyen TA, Koide M, Takahashi T, Shirakashi M (2010) Universality of longitudinal vortices shedding from cruciform two circular cylinder system in uniform flow. *J Fluid Sci* 5(3):603–615. doi:[10.1299/jfst.5.603](https://doi.org/10.1299/jfst.5.603)
- Nguyen TA, Koide M, Yamada S, Takahashi T, Shirakashi M (2012) Influence of mass and damping ratios on VIVs of a cylinder with a downstream counterpart in cruciform arrangement. *J Fluids Struct* 28:40–55. doi:[10.1016/j.jfluidstructs.2011.10.006](https://doi.org/10.1016/j.jfluidstructs.2011.10.006)
- Shirakashi M, Mizuguchi K, Bae HM (1989) Flow-induced excitation of an elastically—supported cylinder caused by another located downstream in cruciform arrangement. *J Fluids Struct* 3(6):595–607. doi:[10.1016/S0889-9746\(89\)90150-3](https://doi.org/10.1016/S0889-9746(89)90150-3)
- Shirakashi M, Bae HM, Sano M, Takahashi T (1994) Characteristics of periodic vortex shedding from two cylinders in cruciform arrangement. *J Fluids Struct* 8(3):239–256. doi:[10.1006/jfls.1994.1012](https://doi.org/10.1006/jfls.1994.1012)
- Shirakashi M, Takahashi T, Kumagai I, Matsumoto T (2001) Vortex-induced vibration of the upstream cylinder of a two-cylinder system in cruciform arrangement. *J Comput Appl Mech* 2(1):103–122
- Takahashi T, Baranyi L, Shirakashi M (1999) Configuration and frequency of longitudinal vortices shedding from two circular cylinders in cruciform arrangement. *J Vis Soc Jpn* 19(75):328–336. doi:[10.3154/jvs.19.75_328](https://doi.org/10.3154/jvs.19.75_328)
- Zdravkovich MM (1983) Interference between two circular cylinders forming a cross. *J Fluid Mech* 128:231–246. doi:[10.1017/S0022112083000464](https://doi.org/10.1017/S0022112083000464)